Collagen Orientation in Periosteum and Perichondrium Is Aligned with Preferential Directions of Tissue Growth

Jasper Foolen,[1] Corrinus C. van Donkelaar,[1] Niamh Nowlan,[2] Paula Murphy,[3] Rik Huiskes,[1] Keita Ito[1]

[1]Biomedical Engineering, Eindhoven University of Technology, WH 4.118, P.O. Box 513, Eindhoven 5600 MB, The Netherlands, [2]Trinity Centre for Bioengineering, School of Engineering, Trinity College, Dublin, Ireland, [3]Department of Zoology, School of Natural Sciences, Trinity College

Received 29 June 2007; accepted 25 October 2007
Published online in Wiley InterScience (www.interscience.wiley.com). DOI 10.1002/jor.20586

ABSTRACT: A feedback mechanism between different tissues in a growing bone is thought to determine the bone's morphogenesis. Cartilage growth strains the surrounding tissues, eliciting alterations of its matrix, which in turn, creates anisotropic stresses, guiding directionality of cartilage growth. The purpose of this study was to evaluate this hypothesis by determining whether collagen fiber directions in the perichondrium and periosteum align with the preferential directions of long bone growth. Tibiotarsi from chicken embryos across developmental stages were scanned using optical projection tomography (OPT) to assess preferential directions of growth at characteristic sites in perichondrium and periosteum. Quantified morphometric data were compared with two-photon laser-scanning microscopy images of the three-dimensional collagen network in these fibrous tissues. The diaphyseal periosteum contained longitudinally oriented collagen fibers that aligned with the preferential growth direction. Longitudinal growth at both metaphyses was twice the circumferential growth. This concurred with well-developed circumferential fibers, which covered and were partly interwoven with a dominant network of longitudinally oriented fibers in the outer layer of the perichondrium/periosteum at the metaphysis. Toward both articulations, the collagen network of the epiphyseal surface was randomly oriented, and growth was approximately biaxial. These findings support the hypothesis that the anisotropic architecture of the collagen network, detected in periosteum and perichondrium, concurs with the assessed growth directions. © 2008 Orthopaedic Research Society. Published by Wiley Periodicals, Inc. J Orthop Res 26:1263–1268, 2008

Keywords: collagen orientation; periosteum; perichondrium; tissue growth

Morphogenesis of developing long bones is the result of cartilage growth. The growing bone is enclosed by the perichondrium in the epiphysis and by the periosteum in the metaphysis and diaphysis. The anisotropy in growth, determining its shape, is believed to be due to the influence of the surrounding tissues, which continuously adapt to the changing mechanical environment. This concept was formulated in the so-called "direction dilation" theory,[1] according to which bone morphogenesis results from the combination of pressure-induced tissue dilation and spatial variations in the resistance against deformation. Ample evidence exists to support this theory. In developing porcine femora, radial expansion only occurs until a perichondrium is formed. From this point longitudinal elongation predominates.[2] In embryonic chicks, the best organized perichondrium is colocalized with the narrowest parts of the developing bone.[3] Disruption of the epiphyseal perichondrium by incision or collagenase treatment results in the development of small protrusions and increased epiphyseal width, respectively.[1,4] The "direction dilation" theory also seems applicable to the periosteum, which spans the metaphyseal and diaphyseal cartilage. Circumferentially cutting the periosteum, just below the epiphysis, enhances longitudinal growth[3,5] and reduces the force (by 80%) needed for epiphysiolysis.[6] Likewise, a hemicircumferential cut induces longitudinal overgrowth at the incised side.[7]

During growth, the volume of cartilage increases, resulting in "growth-generated strains and stresses" in the enclosing tissues.[8] Hence, the cells and extracellular matrix of the perichondrium and periosteum are strained. In turn, because of this external restraint to epiphyseal growth by perichondrium and periosteum, hydrostatic pressure is maintained in the epiphyseal cartilage. Hydrostatic pressure is known to modulate the development of cartilage, through stimulation or inhibition of proliferation and proteoglycan synthesis, depending on the nature of the pressure.[9–11]

If the enclosing tissues would not adapt to the elongation during growth, they would be elongated beyond failure strain. Hence, to allow growth, adaptation of the collagen network in the enclosing tissues is required. The mechanical environment controls fibrous tissue remodeling by regulating the expression and synthesis of collagen,[12–14] the production of proteases,[15] and the alignment of cells and collagen parallel to the strain direction.[16] Additionally, the susceptibility of collagen fibers to enzymatic degradation by collagenase is strain dependent. At an optimal stretch of 4%, collagen degradation is minimized.[17] The diffusion rate of collagenase is not significantly different in 4% strained samples, compared to unloaded controls. Therefore, it is suggested that the degradation pattern depends on altered kinetics of the collagenase–matrix interaction.[18] In favor of this suggestion, it is found that collagen fibrils, perpendicular to the direction of tensile loading, degrade more easily compared to fibrils aligned with the loading direction. This phenomenon is called "strain stabilization."[19] The direction of the load can therefore influence the anisotropy of a collagen network by synthesizing new collagen and degrading existing collagen in a strain-dependent manner. Hereby, a tissue adapts its mechanical properties to the load it experiences.[20]

These mechanisms can explain the alignment of collagen to the direction in which a tissue is strained, which is known to occur in dynamically loaded fibrous tissues. However, it is unknown whether the quasi-static

Correspondence to: C.C. van Donkelaar (T: +31 40 247 3135; F: +31 40 244 7355; E-mail: c.c.v.donkelaar@tue.nl)

© 2008 Orthopaedic Research Society. Published by Wiley Periodicals, Inc.

growth-generated strain can also modulate the direction of a collagen network. Hence, our aims were to determine the 3D collagen orientation in periosteum and perichondrium of embryonic chick tibiotarsi from developmental stages 39 to 40, and to determine whether they are aligned with the directions of growth from stage 38 to 41. This is the first step in validating the concept that a load-dependent feedback mechanism prevails between different tissue types in growing bones.

ANIMALS AND METHODS

Animals

Fertilized eggs of White Leghorn chickens ('t Anker, Ochten, The Netherlands) were placed in a polyhatch incubator (Brisnea). After a 12- to 15-day period of incubation, chick embryos were removed from the eggs and sacrificed by decapitation. This incubation period corresponded to embryos ranging from Hamburger and Hamilton stage 38 to 41.[21] Tibiotarsi were carefully dissected, without damaging periosteum or perichondrium.

Growth by Optical Projection Tomography

For whole-mount staining, 28 tibiotarsi from embryonic day e12 to e15 chicks were fixed immediately upon dissection in 95% ethanol for 4 days at 4°C. The tissue was cleared in 1% potassium hydroxide and stained for 8 h with 0.1% Alcian Blue (Sigma, St. Louis, MO) for cartilage and for 3 h with 0.014% Alizarin Red (Fluka, Milwaukee, Wi) for bone, consecutively. After staining, the tissue was embedded in 1% low melting point agarose (Invitrogen, San Diego, Ca). Embedded samples were dehydrated in 100% methanol and cleared in a solution of benzyl benzoate and benzyl alcohol (2:1; Sigma). Samples were scanned using Optical Projection Tomography (OPT), as described by Sharpe et al.,[22] using a prototype OPT scanning device, constructed at the Medical Research Council Human Genetics Unit (Edinburgh, UK) and installed in the Zoology Dept., Trinity College Dublin. A 3D computer representation of each bone rudiment was produced by integrating 400 serial visible light transmission images from each scanned specimen.[22] The 3D representations could be virtually sectioned in any orientation, and comparable sections were used to measure a total of 10 morphometric parameters (lengths) for each specimen (Fig. 1). Data for each parameter were pooled per embryonic age. A linear regression fit between length and age was taken as the growth rate in mm/day.

Collagen Orientation by Multiphoton Microscopy

Chick tibiotarsi from embryonic day 13 to 14 ($n = 16$) were used for visualization of the perichondrial and periosteal collagen network. Upon dissection, tibiotarsi were incubated in PBS, supplemented with a collagen probe (2.5 μM)[23] for 1 h at 37°C, 5% CO_2. The probe has an inherent specificity for collagen binding protein domains present in integrins ($GST\alpha_1$) and bacterial adhesion proteins (CNA35). It has a high affinity for collagen I, relative to other collagen types and showed very little crossreactivity with noncollagenous extracellular matrix proteins.[23] After incubation, samples were washed in PBS to remove excessive dye and kept in PBS for the remainder of the experiment. During visualization, tibiotarsi were immersed in PBS and put in a chambered coverglass (Lab-Tek II). Both the proximal and distal sides of the bones were examined, using a multiphoton microscope (Zeiss LSM 510 META NLO) in Two-Photon-LSM (TPLSM) mode. The excitation source was a Coherent Chameleon Ultra Ti:Sapphire laser, tuned and mode-locked at 763 nm. This wavelength resulted in the highest intensity profile for the collagen probe. Laser light was focused on the tissue with a Plan-Apochromat 20×/0.8 numerical aperture (NA) objective or C-Apochromat 63×/1.2 NA water objective, connected to a Zeiss Axiovert 200M. The pinhole of the photo-multiplier was fully opened. The photo-multiplier accepted a wavelength region of 500–530 nm. All single images shown in this paper were obtained from Z-stacks, taken through the perichondrium or periosteum. No additional image processing was performed.

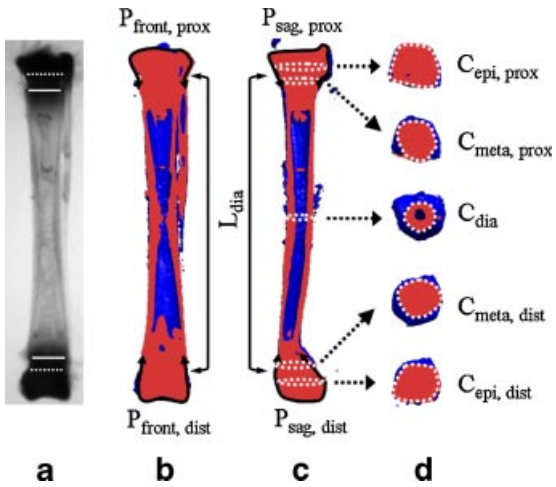

Figure 1. Morphometric parameters from OPT data. (a) Raw OPT image of an e14 chick tibiotarsus. Continuous lines represent the end of the bond shaft where the perichondrium begins, visible in the raw data. Dashed lines represent periosteum attachments to the epiphyses, at the location where the epiphysis widens. (b) Midfrontal and (c) midsagittal sections through the bone, in which perimeter dimensions (P_x) represent the length of the perichondrium in the sagittal and frontal sections, indicted in (c). Circumferential dimensions (C_x) represent the circumference of the perichondrium or periosteum in transverse sections. Light grey areas represent the cut planes of the section and dark grey represents adjacent tissue, located in deeper planes. The longitudinal dimension (L_{dia}) was measured between attachments of the periosteum to the epiphyses [indicated by dashed lines in (a)]. Circumference of the diaphysis (C_{dia}) was measured at the midshaft. Circumference of the distal ($C_{meta,dist}$) and proximal metaphysis ($C_{meta,prox}$) were measured in between the bone shaft and periosteum attachment. Circumference at the distal ($C_{opt,dist}$) and proximal epiphysis ($C_{epi,prox}$) were measured near the largest transverse section. Perimeters of the perichondrium at the proximal epiphysis in the sagittal ($P_{sag,prox}$) and frontal ($P_{front,prox}$) section were measured from the medial to the lateral end of the bone shaft. Corresponding parameters in the distal epiphysis ($P_{sag,dist}$ and $P_{front,dist}$) were measured similarly.

Statistics

Two-way ANOVA was used to determine the effect of the independent variable (embryonic age) and its interaction with morphometric dimensions (L_{dia}, C_{dia}, $C_{meta,\ dist}$, and $C_{meta,\ prox}$; $C_{epi,\ dist}$, $P_{sag,dist}$, and $P_{front,dist}$; $C_{epi,\ prox}$, $P_{sag,prox}$, and $P_{front,prox}$) of the tibiotarsi. If an interaction was found, two-way ANOVA was repeated for individual parameters, and the p-value corrected with the Bonferoni criterion. The p-values of <0.05 were considered significant.

RESULTS

Growth

Growth in the epiphyseal perichondrium is shown in Figure 2. Linear regressions had R^2 values from 0.86 to 0.93. Significant differences were assessed for growth rates in the distal and proximal epiphyses separately. A

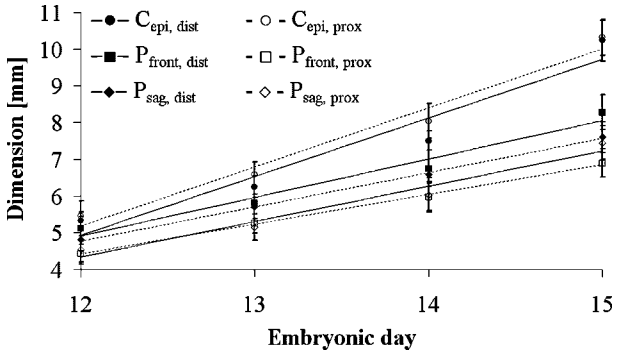

Figure 2. Growth in the epiphysis. Circumferential ($C_{epi,prox}$) and $C_{epi,dist}$) and perimeter dimensions in the frontal and sagittal sections ($P_{sag,dist}$, $P_{sag,prox}$, $P_{front,dist}$, and $P_{front,prox}$) against embryonic age ($n = 28$).

significant difference was found between the slopes (Table 1) of the circumferential parameters ($C_{epi,dist}$ and $C_{epi,prox}$) and the perimeters ($P_{sag,dist}$, $P_{sag,prox}$, $P_{front,dist}$, and $P_{front,prox}$). At both extremities, circumferential growth exceeded growth of the perimeter. The ratio between them ranged from 1.54–1.97 (Table 2). Perimeter growth in both epiphyses ($P_{sag,ankle}$ and $P_{front,dist}$; $P_{sag,prox}$ and $P_{front,prox}$) was not different.

Growth in the metaphysis and diaphysis is shown in Figure 3. Linear regressions had R^2 values from 0.92 to 0.96. A significant difference was found between the slopes (Table 1) of the longitudinal parameter (L_{dia}), all circumferential parameters (C_{dia}, $C_{meta,dist}$, $C_{meta,prox}$), and circumferential growth at both metaphysis ($C_{meta,dist}$, $C_{meta,prox}$) with circumferential growth at the diaphysis (C_{dia}). At the metaphyses, circumferential growth was approximately half the longitudinal growth, whereas at the diaphysis this ratio was 1:4 (Table 2).

Collagen Fiber Orientation

At the diaphysis, the outer layer of the periosteum (Fig. 4B) contained some randomly oriented collagen fibers. Deeper into the tissue (Fig. 4C and D) the orientation was highly anisotropic with almost all fibers oriented longitudinally.

In the metaphysis, the outer layer of the perichondrium was composed of a thin, random fiber network (arrows in Fig. 4F and G). Underneath this layer, thicker circumferential fibers, presumably originating from the perichondrium (dashed circles in Fig. 7F–H Fig. 7), were entangled with longitudinal fibers. The latter, comprising the inner fibrous layer (asterisks in Fig. 4G and H), were continuous with the well-developed longitudinal fibers in the diaphyseal periosteum.

The collagen network in the perichondrium covering the epiphyses had no predominant orientation (Fig. 4J–L), and was therefore considered random. Sporadically, locations were identified where groups of fibers ran in parallel (arrowhead in Fig. 4L). No differences in collagen orientation were observed between the examined tibiotarsi.

An overview of the results is depicted in Figure 5. Longitudinal periosteum fibers spanned the diaphysis and the metaphyses and attached to the epiphyseal base. Growth in the diaphysis was predominantly in the longitudinal direction (ratio of 4:1), and all periosteum fibers aligned with that direction. The outer layer of the

Table 1. Growth Rates in the Diaphysis, Metaphysis and Epiphysis

	Growth rate ± S.D. [mm/day]	R^2
Diaphysis/Metaphysis		
L_{dia}	2.42 ± 0.14	0.92
C_{dia}	0.67 ± 0.03	0.96
$C_{meta,dist}$	1.30 ± 0.07	0.93
$C_{meta,prox}$	1.12 ± 0.05	0.95
Epiphysis distal		
$C_{epi,dist}$	1.60 ± 0.10	0.91
$P_{front,dist}$	1.04 ± 0.08	0.87
$P_{sag,dist}$	0.96 ± 0.08	0.86
Epiphysis proximal		
$C_{epi,prox}$	1.60 ± 0.09	0.93
$P_{front,prox}$	0.81 ± 0.05	0.90
$P_{sag,prox}$	0.93 ± 0.05	0.92

n = 28. Values represent the slopes of the linear regression lines depicted in Figures 1 and 2. *Statistical differences, $p < 0.05$.

Table 2. Growth Ratios Between Growth Rates (Table 1) in the Diaphysis, Metaphysis and Epiphysis (n = 28)

	Growth ratio [–]
Diaphysis/Metaphysis	
$C_{meta,dist}/L_{dia}$	0.54
$C_{meta,prox}/L_{dia}$	0.46
C_{dia}/L_{dia}	0.28
Epiphysis distal	
$C_{epi,dist}/P_{front,dist}$	1.54
$C_{epi,dist}/P_{sag,dist}$	1.67
$P_{sag,dist}/P_{front,dist}$	0.92
Epiphysis proximal	
$C_{epi,prox}/P_{front,prox}$	1.97
$C_{epi,prox}/P_{sag,prox}$	1.72
$P_{front,prox}/P_{sag,prox}$	0.87

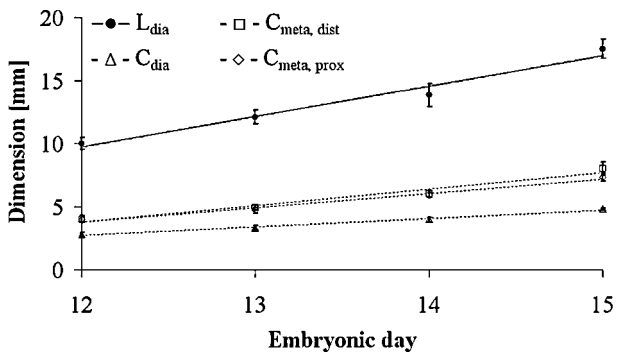

Figure 3. Growth in the metaphysis and diaphysis. Circumferential ($C_{meta,dist}$, $C_{meta,prox}$, and C_{dia}) and longitudinal dimension (L_{dia}) against embryonic age ($n = 28$).

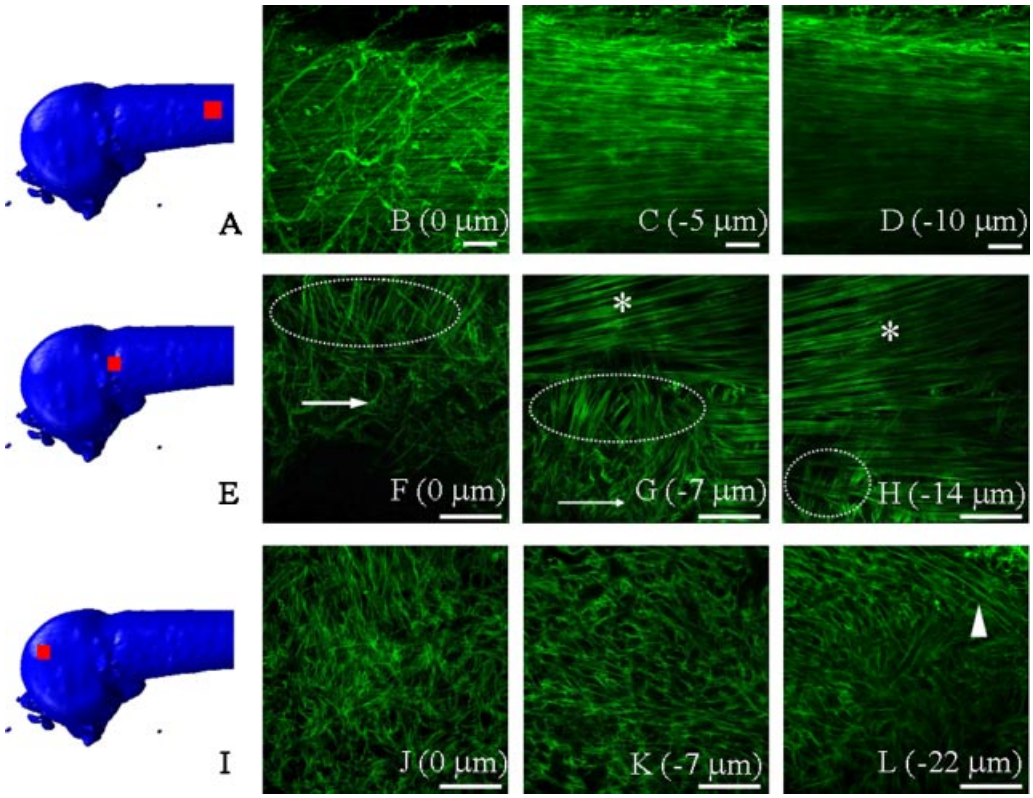

Figure 4. TPLSM images of collagen in the perichondrium and periosteum of an e13 chick tibiotarsus. White squares indicate the location of the z-satck. In (A), the diaphyseal peiosteum, (e) metaphyseal periosteum/perichondrium, and (I) epiphyseal perichondrium. (B–D) Fiber orientation in the diaphyseal periosteum. (B) A thin layer of collagen without a preferentail orientation covers (C) logitudinal collagen fibers. (F–H) Fiber orientation in the metaphyseal periosteum/perichondrium. Asterisk: longitudinal periosteal fibers extending from the diaphysis. Dashed circles: circumferential fibers interwoven with the longitudinally organized deeper network. Arrows: random fiber orientation in the outer layer. (J–L) Fiber orientation in the epiphyseal perichondrium is random. Arrowhead: sparse areas with few parallel fibers. (B–D) Objective 20×, NA 0.8. (F–H and J–l): Objective 63× NA 1.2. Scale bars: 50 μm. Image depth is indicated on images.

perichondrium/periosteum in the metaphysis contained well-developed circumferential fibers that covered, and were partly interwoven with, a dominant network of longitudinally oriented fibers. Longitudinal metaphyseal growth was twice the circumferential growth. Toward the articulations, the collagen network of the epiphyseal surface was randomly oriented and growth was approximately equibiaxial at both the distal and proximal sides.

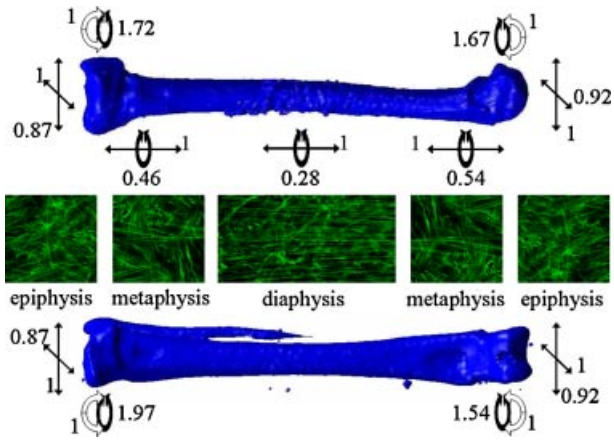

Figure 5. Overview of normalized growth ratios (see Table 2) and corresponding collagen orientation in the diaphysis, metaphysis, and epiphysis of the developing tibiotarsus (e13–e14). Sagittal view on top, frontal view below. Proximal left, distal right.

DISCUSSION

The 3D collagen orientation in embryonic chick tibiotarsi periosteum and perichondrium were compared to the directions of tibiotarsi growth. The results (Fig. 5) revealed that epiphyseal growth was isotropic at the bone–extremity surfaces, whereas at the epiphyseal center, circumferential growth dominated. This corresponded to a random collagen network in the epiphyseal perichondrium. Longitudinal periosteum fibers spanned the metaphysis and diaphysis, and aligned with the dominant longitudinal growth in the diaphysis. Circumferential growth was larger at the metaphysis compared to the diaphysis, which concurred with the finding that longitudinal fibers were covered by a layer of circumferentially oriented fibers at the metaphysis, but not at the diaphysis. The biaxial collagen network of the metaphysis was found to originate from the dominant longitudinally oriented periosteal fibers at the diaphysis. These fibers were continuous, with fibers at both metaphyses, and were fixed at the epiphyseal base only. Adhesion of the periosteum to the underlying cartilage and bone at other locations was poor.[24] The longitudinal fibers spanned the complete metaphysis and diaphysis,

and were loaded in this direction. Their insertions are unfavorable for acting against circumferential growth; therefore, another sheet of fibers was found perpendicular to the longitudinal direction. These finding support our hypothesis that predominant directions of growth, generate strain in corresponding directions, which aligns collagen fibers in the perichondrium and periosteum. Hence, growth is proposed to trigger collagen–fiber orientation.

We compared growth at characteristic sites to local orientations of collagen at corresponding sites. A limitation to this study is that the exact location of the TPLSM scans cannot be assessed. It remains experimentally challenging to compare detailed quantified growth at a small scale with collagen orientations at matching locations.

This study shows that collagen orientation coincides with the ratio between different directions of absolute growth (in mm/day). However, growth is defined as a combination of tissue strain and remodeling. The actual strain the collagen fibers experience, which is the genuine trigger for collagen alignment, may differ from the growth rate. Knowledge of such would provide additional insight in the mechanism of collagen turnover by mechanical stimulation. One preliminary study[25] estimated residual strain in middiaphyseal periosteum of similarly aged chicks as high as 105% in the longitudinal direction and 10% in the circumferential direction.

In 7- to 8-week-old rabbit metatarsals, collagen orientation in the periosteum–perichondrium is predominantly longitudinal, with some distinct groups of fibers lying in a circumferential orientation or oblique to the long axis.[26] The periosteum of the rabbit femur also displayed longitudinally oriented collagen fibers.[27] In ribs of 5-month-old rabbits, collagen is oriented parallel to the longitudinal axis of the rib, while in the outer zone of the cartilage, collagen layers are mostly arranged circumferentially.[28] The observations in these studies are in agreement with fiber orientations found in the present study. In a crossbreed of New Hampshire and Barred Rock chickens, growth in length and diaphyseal diameter of tibias is linear during the first 3 weeks after fertilization.[29] All corresponding growth dimensions in this crossbreed exceed those of the White-Leghorn chickens from this study by a factor of approximately 2. However, the linear increase of the bone dimensions during the second week after fertilization is in agreement with this study. To the knowledge of the authors, collagen orientation has never been related to growth directions in developing tissues.

Many studies[16–19,30–34] relate mechanical load to direction dependent degradation and alignment of collagen. The orientation of collagen has been assessed in fibroblast-seeded collagen gels, subjected to different loading regimes. Unloaded gels display a disorganized collagen distribution.[16] Uniaxially constrained gels develop high degrees of fiber alignment and mechanical anisotropy, while collagen gels constrained biaxially remain mechanically isotropic with randomly distributed collagen fibers.[16,35] Using the same setup, static uniaxial load induces greater ultimate stress and material modulus compared to dynamic load.[20] Differences in collagen alignment between statically and dynamically loaded samples have not been reported. Compaction force of the tethered collagen samples increased immediately, reaching a maximum after 2 days of culturing.[36] These studies all suggest a relation between strain and collagen orientation; however, they do not indicate what the relation implies.

Driessen et al.[37] hypothesized that collagen fibers align with the direction in between the principal tensile strains, dependent on the strain magnitudes. Predited collagen architectures with this theory concur with the collagen orientation in various dynamically loaded tissues, including heart valves,[38] blood vessels,[37] and articular cartilage.[39] The present paper shows that collagen orientations in the perichondrium and periosteum align with the directions of growth. Growth is a combination of mechanical tissue strain and the synthesis of new tissue matrix. Exactly how growth relates to mechanical tissue strain is yet unknown. Hence, it is difficult to correlate the measured collagen orientation in periosteum and perichondrium to predictions by these theories. Possibly the mechanism for collagen orientation is different in growing tissues that are quasi-statically loaded, compared to dynamically loaded tissues.

We conclude that the local anisotropy in the periosteum and perichondrium concurs with preferential growth directions. This agrees with the concept that a load-dependent feedback mechanism prevails between different tissue types in growing bones.

ACKNOWLEDGMENTS

We gratefully acknowledge Kristen Summerhurst from Trinity College, Dublin, for help in the use of OPT. This project is funded by the Royal Netherlands Academy of Arts and Sciences.

REFERENCES

1. Wolpert L. 1981. Cartilage morphogenesis in the limb. In: Bellairs R, Curtis ASG, Dunn G, editors. Cell behaviour. Longon: Cambridge Univ. Press; p 359–372.
2. Carey EJ. 1922. Direct observations on the transformations of the mesenchyme in the thigh of the pig embryo, with especial reference to the genesis of the thigh muscles of the knee and hip joints, and of the primary bone of the femur. J Morphol Physiol 37:1–77.
3. Rooney P, Archer CW. 1992. The development of the perichondrium in the avian ulna. J Anat 181(Pt 3):393–401.
4. Rooney P. 1984. The cellular basis of cartilage morphogenesis in embryonic chick limbs. PhD thesis, University of London.
5. Crilly RG. 1972. Longitudinal overgrowth of chicken radius. J Anat 112:11–18.
6. Shapiro F. 2001. Pediatric orthopedic deformities, basic science, diagnosis, and treatment. San Diego, CA: Elsevier/Academic Press.
7. Dimitriou CG, Kapetanos GA, Symeonides PP. 1988. The effect of partial periosteal division on growth of the long bones. An experimental study in rabbits. Clin Orthop Relat Res 236: 265–269.

8. Henderson JH, Carter DR. 2002. Mechanical induction in limb morphogenesis: the role of growth-generated strains and pressures. Bone 31:645–653.
9. Hall AC, Urban JP, Gehl KA. 1991. The effects of hydrostatic pressure on matrix synthesis in articular cartilage. J Orthop Res 9:1–10.
10. Hansen U, Schunke M, Domm C, et al. 2001. Combination of reduced oxygen tension and intermittent hydrostatic pressure: a useful tool in articular cartilage tissue engineering. J Biomech 34:941–949.
11. Parkkinen JJ, Ikonen J, Lammi MJ, et al. 1993. Effects of cyclic hydrostatic pressure on proteoglycan synthesis in cultured chondrocytes and articular cartilage explants. Arch Biochem Biophys 300:458–465.
12. Kim SG, Akaike T, Sasagaw T, et al. 2002. Gene expression of type I and type III collagen by mechanical stretch in anterior cruciate ligament cells. Cell Struct Funct 27:139–144.
13. Parsons M, Kessler E, Laurent GJ, et al. 1999. Mechanical load enhances procollagen processing in dermal fibroblasts by regulating levels of procollagen C-proteinase. Exp Cell Res 252:319–331.
14. Yang G, Crawford RC, Wang JHC. 2004. Proliferation and collagen production of human patellar tendon fibroblasts in response to cyclic uniaxial stretching in serum-free conditions. J Biomech 37:1543–1550.
15. Prajapati RT, Chavally-Mis B, Herbage D, et al. 2000. Mechanical loading regulates protease production by fibroblasts in three-dimensional collagen substrates. Wound Repair Regen 8:226–237.
16. Henshaw DR, Attia E, Bhargava M, et al. 2006. Canine ACL fibroblast integrin expression and cell alignment in response to cyclic tensile strain in three-dimensional collagen gels. J Orthop Res 24:481–490.
17. Huang C, Yannas IV. 1977. Mechanochemical studies of enzymatic degradation of insoluble collagen fibers. J Biomed Mater Res 11:137–154.
18. Nabeshima Y, Grood ES, Sakurai A, et al. 1996. Uniaxial tension inhibits tendon collagen degradation by collagenase in vitro. J Orthop Res 14:123–130.
19. Ruberti JW, Hallab NJ. 2005. Strain-controlled enzymatic cleavage of collagen in loaded matrix. Biochem Biophys Res Commun 336:483–489.
20. Feng Z, Tateishi Y, Nomura Y, et al. 2006. Construction of fibroblast-collagen gels with orientated fibrils induced by static or dynamic stress: toward the fabrication of small tendon grafts. J Artif Organs 9:220–225.
21. Hamburger V, Hamilton HL. 1992. A series of normal stages in the development of the chick embryo. 1951. Dev Dyn 195: 231–272.
22. Sharpe J, Ahlgren U, Perry P, et al. 2002. Optical projection tomography as a tool for 3D microscopy and gene expression studies. Science 296:541–545.
23. Krahn KN, Bouten CVC, van Tuijl S, et al. 2006. Fluorescently labeled collagen binding proteins allow specific visualization of collagen in tissues and live cell culture. Anal Biochem 350:177–185.
24. Bertram JE, Polevoy Y, Cullinane DM. 1998. Mechanics of avian fibrous periosteum: tensile and adhesion properties during growth. Bone 22:669–675.
25. Chen JC, Zhao B, Longaker MT, et al. 2007. Periosteal biaxial residual stresses and strains during chick embryonic bone growth. 53rd annual meeting of the Orthopaedic Research Society, San Diego; abstract number 1333.
26. Speer DP. 1982. Collagenous architecture of the growth plate and perichondrial ossification groove. J Bone Joint Surg Am 64:399–407.
27. Dejonge P. 1983. Collagen-fibers in the periosteum of a long bone. Acta Morphol Neerlando-Scand 21:173–174.
28. Bairati A, Comazzi M, Gioria M. 1996. A comparative study of perichondrial tissue in mammalian cartilages. Tissue Cell 28:455–468.
29. Church LE, Johnson LC. 1964. Growth of long bones in the chicken. Rates of growth in length and diameter of the humerus, tibia and metatarsus. Am J Anat 114:521–538.
30. Caruso AB, Dunn MG. 2004. Functional evaluation of collagen fiber scaffolds for ACL reconstruction: cyclic loading in proteolytic enzyme solutions. J Biomed Mater Res A 69:164–171.
31. Ellsmere JC, Khanna RA, Lee JM. 1999. Mechanical loading of bovine pericardium accelerates enzymatic degradation. Biomaterials 20:1143–1150.
32. Guidry C, Grinnell F. 1985. Studies on the mechanism of hydrated collagen gel reorganization by human skin fibroblasts. J Cell Sci 79:67–81.
33. Sawhney RK, Howard J. 2002. Slow local movements of collagen fibers by fibroblasts drive the rapid global self-organization of collagen gels. J Cell Biol 157:1083–1091.
34. Wang JHC, Jia F, Gilbert TW, et al. 2003. Cell orientation determines the alignment of cell-produced collagenous matrix. J Biomech 36:97–102.
35. Thomopoulos S, Fomovsky GM, Holmes JW. 2005. The development of structural and mechanical anisotropy in fibroblast populated collagen gels. J Biomech Eng 127:742–750.
36. Feng Z, Ishibashi M, Nomura Y, et al. 2006. Constraint stress, microstructural characteristics, and enhanced mechanical properties of a special fibroblast-embedded collagen construct. Artif Organs 30:870–877.
37. Driessen NJB, Wilson W, Bouten CVC, et al. 2004. A computational model for collagen fibre remodelling in the arterial wall. J Theor Biol 226:53–64.
38. Driessen NJB, Bouten CVC, Baaijens FPT. 2005. Improved prediction of the collagen fiber architecture in the aortic heart valve. J Biomech Eng 127:329–336.
39. Wilson W, Driessen NJB, van Donkelaar CC, et al. 2006. Prediction of collagen orientation in articular cartilage by a collagen remodeling algorithm. Osteoarthritis Cartilage 14: 1196–1202.